Metabolic engineering of β-oxidation to leverage thioesterases for production of 2-heptanone, 2-nonanone and 2-undecanone

Qiang Yan[a,b,1], Trevor R. Simmons[a,1], William T. Cordell[a,b], Néstor J. Hernández Lozada[a], Christian J. Breckner[a], Xuanqi Chen[a], Michael A. Jindra[a], and Brian F. Pfleger [a,b,c,*]

[a] Department of Chemical and Biological Engineering, University of Wisconsin-Madison, Madison, WI 53706, United States

[b] DOE Center for Advanced Bioenergy and Bioproducts Innovation, University of Wisconsin-Madison, Madison, WI 53706, United States

[c] Microbiology Doctoral Training Program, University of Wisconsin-Madison, Madison, WI 53706, United States

[1] Designates authors contributing equally to the manuscript.

* Corresponding author. 3629 Engineering Hall, 1415 Engineering Drive, Madison, WI 53706, United States. Phone: +1 608 890 1940. Fax: +1 608 262-5434. E-mail address: pfleger@engr.wisc.edu.

Abstract:

Medium-chain length methyl ketones are potential blending fuels due to their cetane numbers and low melting temperatures. Biomanufacturing offers the potential to produce these molecules from renewable resources such as lignocellulosic biomass. In this work, we designed and tested metabolic pathways in *Escherichia coli* to specifically produce 2-heptanone, 2-nonanone and 2-undecanone. We achieved substantial production of each ketone by introducing chain-length specific acyl-ACP thioesterases, blocking the β-oxidation cycle at an advantageous reaction, and introducing active β-ketoacyl-CoA thioesterases. Using a bioprospecting approach, we identified fifteen homologs of *E. coli* β-ketoacyl-CoA thioesterase (FadM) and evaluated the *in vivo* activity of each against various chain length substrates. The FadM variant from *Providencia sneebia* produced the most 2-heptanone, 2-nonanone, and 2-undecanone, suggesting it has the highest activity on the corresponding β-ketoacyl-CoA substrates. We tested enzyme variants, including acyl-CoA oxidases, thiolases, and bi-functional 3-hydroxyacyl-CoA dehydratases to maximize conversion of fatty acids to β-keto acyl-CoAs for 2-heptanone, 2-nonanone, and 2-undecanone production. In order to address the issue of product loss during fermentation, we applied a 20% (v/v) dodecane layer in the bioreactor and built an external water cooling condenser connecting to the bioreactor heat-transferring condenser coupling to the condenser. Using these modifications, we were able to generate up to 4.4 g/L total medium-chain length methyl ketones.

Graphic Abstract:

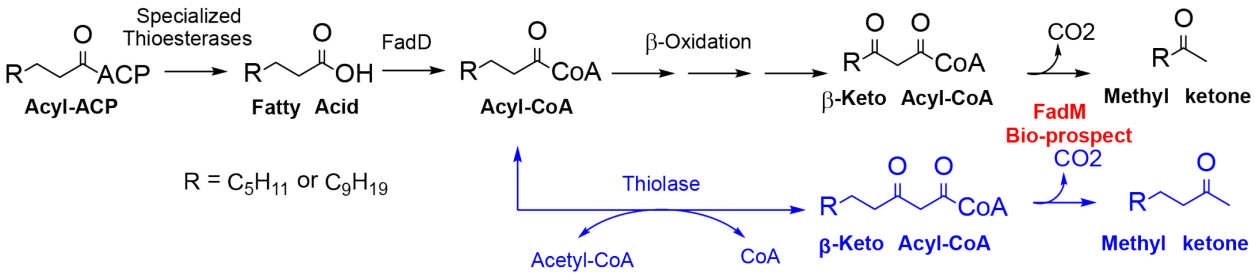

Engineering β-Oxidation to Leverage Thioesterases for Methyl Ketone Synthesis

Highlights:

- β-oxidation and thiolase-mediated routes used to produce medium-chain methyl ketones
- Bio-prospecting identified FadM homolog from *Providencia sneebia* with higher activity
- We report production of highest medium-chain MKs titers, 4.4 g/L

Keywords: thioesterase; 2-heptanone; 2-nonanone; 2-undecanone; thiolase; metabolic engineering

1. Introduction

Methyl ketones (MK) are naturally occurring compounds that have been shown to serve biological and industrial functions such as insecticides, pheromones, flavors, and fragrances, e.g. blue cheese flavor and fragrance comes from 2-heptanone and 2-nonanone produced by fungus in the maturation process (Collins et al., 2003). Similarly, 2-heptanone, 2-nonanone, 2-undecanone are found in plants, such as cinnamon, clove and coconut, where they contribute to the insecticide, flavor and fragrance profile (Forney and Markovetz, 1971; Kennedy, 2003; Zhu et al., 2018). Methyl ketones also have the potential to serve as renewable liquid transportation fuels. Medium-chain methyl-ketones, such as 2-nonanone and 2-undecanone, have high cetane numbers and low freezing points, making them compatible with diesel fuels (**Table 1**). In addition, these ketones and 2-heptanone can be condensed to yield long-chain, high cetane fuels (Frias et al., 2011; Harrison and Harvey, 2018).

Table 1 Properties of methyl ketone and its derivatives as potential diesel fuel applications.

	Cetane Number[a]	Melting Temperature[b] (°C)	Citations
2-heptanone	30.0	-35.5	(Yanowitz et al., 2017)
2-nonanone	46.1	-15	(Yanowitz et al., 2017)
2-undecanone	56.5	15	(Goh et al., 2012)
2-tridecanone	60	30.5	(Harrison and Harvey, 2018)
dioxolanes[c]	81-91	-11	(Harrison and Harvey, 2018)
Palm oil derived biodiesel[d]	61.9	13	(Hoekman et al., 2012)
No. 2 petroleum diesel[e]	45	-18	(Hoekman et al., 2012)

[a] Literature reported cetane values that are either characterized experimentally or predicted by models; the minimum cetane number of diesel fuels in the U.S. is 40 according to ASTM standard D975.
[b] Melting temperatures are obtained from a chemical information collection, PubChem (https://pubchem.ncbi.nlm.nih.gov/). In general, the freezing point trend is proportional to the melting temperature trend since both are measuring the required temperature of solid-liquid transition.
[c] The dioxolanes properties reported from the literature exemplified methyl ketones can be condensed to higher energy molecules.
[d] palm oil derived biodiesel is an example of commonly used biodiesel.
[e] No. 2 petroleum diesel is an example of commercial diesel fuels.

Methyl ketones are biologically produced from β-keto acids, unstable compounds that can spontaneously undergo decarboxylation under mild conditions (Kornberg et al., 1948). The medium chain β-keto acids, e.g. 3-oxooctanoate, are relatively less stable than shorter chain

compounds, e.g. acetoacetate, possibly because the pentanyl moiety of 3-oxooctanoate is more favorable for attracting a proton to form a cyclic six-atom transition state of the decarboxylation process than methyl moiety of acetoacetate. This could explain why acetoacetate decarboxylase is an essential and rate-limiting step in acetone (Lan et al., 2013) or 2-butanone (Mehrer et al., 2019; Srirangan et al., 2016) biosynthesis while methyl ketone decarboxylase was shown to be unnecessary for 2-tridecanone biosynthesis (Goh et al., 2012) .

β-keto acids are made via transthioesterification or hydrolysis reactions on β-ketoacyl thioester (-CoA, -ACP) substrates. For example, methyl ketone synthases act either as distinct enzymes (^{Sh}Mks1/2) or as an embedded domain in modular type I polyketide synthases (PKS) by hydrolyzing β-ketoacyl-acyl carrier protein (ACP) substrates (Yu et al., 2010; Yuzawa et al., 2017). Similarly, β-ketoacyl-CoA thioesterases produce β-keto acids via hydrolysis. The long-chain β-keto acids spontaneously decarboxylate to yield methyl ketones (Goh et al., 2014; Nie et al., 2008). Alternatively, β-ketoacyl-CoA transferase (PcalJ) transfers the CoA moiety from short-chain substrates to succinate to form succinyl-CoA and the corresponding β-keto acid. The latter is enzymatically converted to a methyl ketone by acetoacetate decarboxylase (Adc) (Lan et al., 2013).

Over the last decade, several groups have applied metabolic engineering strategies to bacteria and yeast with the goal of increasing flux to desired methyl ketones. For instance, Zhu et al., built a chimeric *Saccharomyces cerevisiae* type I fatty acid synthase (FAS) by embedding a ^{Sh}Mks2 next to an ACP domain to increase the cleavage activities. An engineered strain that co-expressed ^{Sh}Mks1 and the FAS genes produced ~20 μg/g DCW C_{11}-C_{15} methyl ketones (Zhu et al., 2017). Using *Escherichia coli* as a host, Goh et al., compared pathway efficiencies between the acyl-CoA methyl ketone synthase ^{Ec}FadM and the acyl-ACP methyl ketone synthase ^{Sh}MKS1

and ^{Sh}MKS2. The best strain (EGS895) overexpressed β-ketoacyl-CoA thioesterase (^{Ec}FadM), acyl-CoA oxidase (Mlut_11700), acyl-ACP thioesterase (^{Ec}'TesA), and a bifunctional hydratase and dehydrogenase (^{Ec}FadB). This strain produced significantly higher 2-tridecanone than that of the ^{Sh}MKS2 overexpression strain (Goh et al., 2012). In a follow-up study, the authors increased the C_{11}-C_{15} methyl ketone titer up to 3.4 g/L in a fed-batch fermentation by overexpressing native FadR and FadD, deleting key acetate forming pathways, and consolidating the pathway from two plasmids into one (Goh et al., 2014). In addition, the authors further improved the methyl ketone titer up to 5.4 g/L by overexpression of NADH-dependent β-ketoacyl-ACP reductase FabG from *Acholeplasma laidlawii* to mitigate the NADPH imbalance caused by the endogenous FabG (Goh et al., 2018). Thus far, the FadM pathway is the most frequently used pathway for methyl ketone production due to its high activity. Recent efforts have focused on transferring methyl ketone pathways into non-model organisms such as oleaginous yeast, *Yarrowia lipolytica* (Hanko et al., 2018), soil bacteria, *Pseudomonas putida* (Dong et al., 2019) and chemolithoautotrophs, *Ralstonia eutropha* (Muller et al., 2013). Other studies designed metabolic pathways to make shorter chain-length methyl ketones. For instance, Lan et al., constructed an *E. coli* strain that overexpressed *Ralstonia eutropha* thiolase BktB and *Pseudomonas putida* 3-oxoadipate CoA-succinyl transferase PcaIJ. The strain produced ~240 mg/L 2-pentanone from ~12 g/L glucose (Lan et al., 2013). Yuzawa et al., engineered a type I modular polyketide synthase (PKS) to produce short chain methyl ketones by inactivating the ketone reductase (KR) domain and switching to a malonyl-CoA preferred acyltransferase homologue domain. When the engineered PKS was overexpressed in *Streptomyces albus,* the culture generated ~140 mg/L 2-butanone and 2-pentanone (Yuzawa et al., 2018). Although various protein engineering strategies have been applied to control chain-length specificities for oleochemicals such as fatty acids (Yan and Pfleger,

2019), few studies have been reported for the production of 2-heptanone, 2-nonanone, or 2-undecanone (Park et al., 2012; Zhu et al., 2019).

In this manuscript, we describe efforts to engineer *E. coli* to produce medium-chain length methyl ketones. Our work leverages highly-active and selective thioesterases that target 8- and 12-carbon substrates as well as two routes of converting fatty acids to the β-keto acid precursors of our target products. In prior work, we isolated a C_8-specific *Cuphea palustris* FatB1 thioesterase variant, annotated as CpFatB1.2-M4-287, hereafter CpFatB1*, that exhibited a 15-fold increase in k_{cat} compared to the native variant while maintaining >90% selectivity towards producing octanoic acid (Hernández Lozada et al., 2018). An engineered *E. coli* strain that overexpressed the CpFatB1* from a single chromosomal copy produced 1.7 g/L octanoic acid from 20 g/L glycerol. In other studies, we leveraged the C_{12}-specific thioesterase from *Umbellularia californica* (BTE) to produce dodecanoic acid and other 12-carbon oleochemicals at ~g/L titers (Lennen et al., 2010; Agnew et al., 2012; Youngquist et al., 2013). Here, we used the selectivity of these thioesterases and permissive acyl-CoA synthetases to generate pools of acyl-CoAs with narrow chain-length distributions. We then compared a thiolase-mediated condensation and a β-oxidation pathway (**Figure 1**) for generating β-ketoacyl-CoAs with similar chain-length distributions. In order to maximize conversion to methyl ketones, we compared fifteen homologs of the *E. coli* methyl ketone synthase FadM in search of variants with higher activities to medium chain substrates. Lastly, we used a condenser and dodecane overlay to capture volatilized methyl ketones from a bioreactor, thereby achieving the highest reported 2-heptanone titer in a fed-batch fermentation.

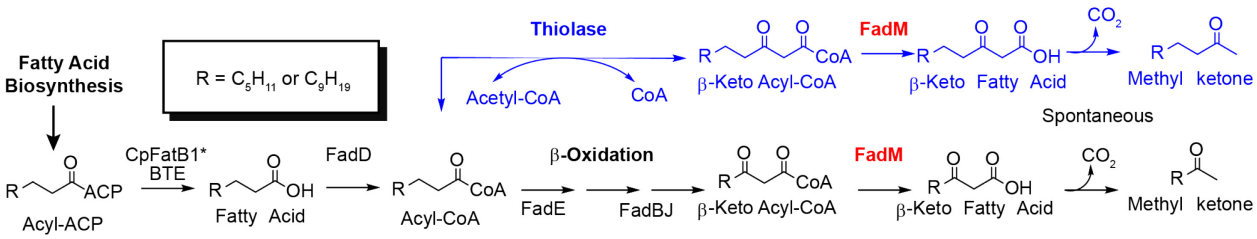

Figure 1 Metabolic pathways designed for producing 2-heptanone, 2-nonanone and 2-undecanone in *E. coli*. Each pathway starts with a C_8- or C_{12}-specific thioesterases (CpFatB1* or BTE) which makes octanoate or dodecanoate from fatty acid biosynthesis. Free fatty acids are reactivated to octanoyl-CoA or dodecanoyl-CoA by fatty acid synthetases (^{Mt}FadD6 or ^{Ec}FadD), respectively. Octanoyl-CoA or dodecanoyl-CoA undergoes an oxidation process by an acyl-CoA dehydrogenase (^{Ec}FadE), and a bi-functional enoyl-CoA hydratase/3-hydroxyacyl-CoA dehydrogenase ^{Ec}FadBJ to generate β-keto-octanoyl-CoA or β-keto-dodecanoyl-CoA (pathways as marked in black). Alternatively, octanoyl-CoA and acetyl-CoA are condensed to generate β-ketodecanoyl-CoA by a thiolase ^{Ec}FadA (marked in blue). The β-ketoacyl-CoAs are converted to β-keto acids by a methyl ketone synthase ^{Ec}FadM (marked in red), then spontaneously decarboxylated to methyl ketones.

2. Materials and Methods

2.1. Bacterial strains, plasmids, oligonucleotides, and reagents

All bacterial strains used in this study are listed in **Supplementary Table 1**. Phusion DNA Polymerase was purchased from New England Biolabs (Ipswich, MA). Plasmid extractions were performed with QIAGEN (Valencia, CA) miniprep reagents. DNA, including oligonucleotide primers and short gBlocks, was synthesized by Integrated DNA Technologies (IDT), Inc. (San Diego, CA). Fatty acids and methyl ketone standards used in this study were purchased from Sigma-Aldrich (St. Louis, MO).

E. coli DH5α cells were used for cloning and assembling DNA molecules. Lysogeny broth (LB) was used to cultivate cells during the cloning and DNA assembly process. *E. coli* NHL17 (K12 MG1655 *ΔaraBAD ΔfadD::trcCpFatB1**), *E. coli* ΔRABIJ (MG1655 *ΔaraBAD ΔfadR ΔfadA ΔfadB ΔfadI ΔfadJ*) and *E. coli* TY34 (MG1655 *ΔaraBAD ΔfadE::*P_{trc}-

BTE ΔfadAB::P_{trc}-BTE ΔackApta::P_{trc}-BTEΦ(P_{trc}-fadD)) were created as part of prior studies (Agnew et al., 2012; Hernández Lozada et al., 2018; Youngquist et al., 2013) and were used as base strains for production of 2-heptanone (NHL17), 2-nonanone (ΔRABIJ) and 2-undecanone (TY34). Pre-cultures were prepared in test tubes containing 5 mL LB and the appropriate antibiotics (final concentrations: carbenicillin, 100 μg/mL; chloramphenicol, 34 μg/mL; kanamycin 50 μg/mL).

2.2. Plasmid and strain construction

All plasmids used in this study are summarized in **Supplementary Table 1**. Plasmid maps are available as Supplementary Materials. Cloning of native *E. coli* genes into expression plasmids was performed by PCR amplification using the primers listed in the supplementary plasmid maps. Plasmids were constructed by annealing linearized DNAs using an isothermal assembly method (Gibson et al., 2009). Chromosomal expression cassettes were created using a combination of lambda red recombination and CRISPR/Cas9-mediated selection as described in prior work (Hernández Lozada et al., 2018; Mehrer et al., 2018). All cloned sequences, integration cassettes, and gene deletions were confirmed by Sanger sequencing performed by Functional Biosciences (Madison, WI).

Sequences of FadM homologs were acquired from the Thyme database (http://www.enzyme.cbirc.iastate.edu/) (Cantu et al., 2011). Protein similarities were performed using the BLAST alignment tool from NCBI. Terminal signal peptide sequences were identified using SignalP 3.0 (http://www.cbs.dtu.dk/services/SignalP-3.0/) (Dyrløv Bendtsen et al., 2004) and were subsequently truncated when genes were designed for synthesis. Constructs expressing FadA and FadB homologs were obtained from a prior study (Mehrer et al., 2018). Genes encoding

FadM homologs, ^{Re}BktB and ^{Ml}ACO were codon-optimized and DNA sequences were chemically synthesized as gBlocks (IDT DNA).

2.3. Characterization of FadM activity in vivo

The relative activity of FadM homologs on various chain length substrates was measured by feeding free fatty acids to cultures of *E. coli* cells expressing a FadM homolog. These cultures were inoculated to starting OD_{600} of 0.05 in 50 mL of LB supplemented with a defined amount of saturated fatty acid. All fatty acids were pre-dissolved in ethanol and supplemented to cultures at the following final concentrations: 1 g/L octanoic acid, 1 g/L decanoic acid, 200 mg/L dodecanoic acid, 100 mg/L tetradecanoic acid, or 100 mg/L hexadecenoic acid. Cultures were then grown at 37°C with shaking at 250 rpm until an OD_{600} of approximately 0.2 was reached. At this point, cultures were supplemented with a final concentration of 1 mM IPTG and cultivated at 30°C with shaking at 250 rpm for an additional 24 h. After induction, samples were taken periodically to measure titers of fatty acids and methyl ketones.

2.4. Methyl ketone production in shake flasks

To demonstrate methyl ketone production in shake flasks, overnight cultures of *E. coli* strains (**Supplementary Table 1**) were inoculated to a starting OD_{600} of 0.05 in Clomburg medium (Clomburg et al., 2012) with 10% (v/v) dodecane and appropriate antibiotics and incubated at 37°C with shaking at 250 rpm. Once the cultures reached an OD_{600} of approximately 0.2, cultures were supplemented to a final concentration of 1 mM IPTG and incubated for an additional 24 hours at 30°C with shaking at 250 rpm.

2.5. Extraction and Quantification of methyl ketones and fatty acids

Fatty acids and methyl ketones were extracted from culture according to an acid-based esterification method described previously (Grisewood et al., 2017; Hernández Lozada et al., 2018). Individual species were separated using a Shimadzu GC equipped with an Agilent RTX-5 column (Santa Clara, CA) and quantified by FID. Quantification of fatty acids was normalized by inclusion of 50 µL of 12.5 mg/mL nonanoic acid, and/or 1.25 mg/mL pentadecanoic acid internal standards dissolved in ethanol. Octanoic acid, decanoic acid and dodecanoic acid were quantified based on the nonanoic acid internal standard, and tetradecanoic acid and hexadecenoic acid were quantified based on the pentadecanoic acid. Quantification of methyl ketones was normalized by inclusion of 50 µL of 62.5 mg/mL 2-octanone and/or 62.5 mg/mL 2-dodecanone dissolved in ethanol. 2-heptanone and 2-nonanone were quantified by 2-octanone, and 2-undecanone and longer chain methyl ketones were quantified by 2-dodecanone. In order to evaluate methyl ketone concentration in the distinct organic or aqueous phases, 50 mL cell cultures were centrifuged at 4500 × *g* for 10 min and 0.5 mL samples from the dodecane layer and 2.5 mL samples aqueous phase were collected and evaluated separately.

To test for the rates of methyl ketone evaporation in our culturing apparatus, a final concentration of ~5.0 g/L 2-heptanone, 3.5 g/L 2-nonanone, and 6 g/L 2-undecanone was dissolved in 50 mL LB medium in 250 mL shake flasks. The concentration of each species was monitored for 48-hours during which the flasks were incubated at 30°C with shaking at 250 rpm. In order to evaluate the effect of dodecane for reducing methyl ketone loss, 10 - 20% (v/v) dodecane was added to flasks and the 2-heptanone, 2-nonanone and 2-undecanone titers were measured every 12 hrs. MK standards (manufacturer) were run at the following concentrations to generate a peak area-based standard curve: 1000 mg/L, 500 mg/L, 250 mg/L, 100 mg/L, 50 mg/L, 25 mg/L.

2.6. Fed-batch bioreactor fermentation

Fed-batch cultivation was performed using a 1-L Infors Multifors bioreactor. Overnight pre-cultures were inoculated to an initial OD_{600} of 0.05 into a bioreactor containing 500 mL Clomburg medium with ~65 g/L glycerol. The bioreactor was operated at the following conditions: temperature was controlled at 30°C at post-induction, air flow was 1.5 L/min, stirrer rate was varied between 250 rpm and 1000 rpm to control dissolved oxygen at a value of 40%, pH was maintained at 7.0 using 3 M phosphoric acid and pure ammonia hydroxide. When the OD_{600} reached 0.2, IPTG was added to achieve a final concentration of 1 mM and 100 mL dodecane was fed in the bioreactor. At 24 h of post-induction, ~500 g/L glycerol was one-time bolus-fed into the bioreactor and fermentation terminated 96 h post-induction. Measurements of methyl ketone, fatty acid, glycerol, optical density, and CO_2 evolution were recorded for 96 hrs total.

The bioreactor outlet gas stream was directed through a heat exchange system to condense methyl ketone vapors stripped from the culture broth. The condenser was constructed with coiled quarter-inch outer diameter stainless steel tubing to ensure sufficient residence time in a water-ice bath. A water chiller supplied 6°C to the outer shell of the condenser. The condensate was channeled to a bored-through union to facilitate the collection of the liquefied sample from the gaseous effluent.

2.7. Analysis of glycerol consumption

Glycerol was quantified on an HPLC (Shimadzu) equipped with an autosampler, quaternary pump, degasser and a refractive index detector. 1 mL fermentation broth samples were prepared by centrifuging at 15,000 × *g*, and filtering the supernatant through a 0.22 μm membrane filter. For each sample, 10 μL was injected and separated for 25 min on a Restek Organic Acids column with a mobile phase of 5 mM H_2SO_4 at a flow rate of 0.6 mL/min. Glycerol standards

(manufacturer) were run at the following concentrations to generate a peak area-based standard curve: 100 g/L, 50 g/L, 25 g/L, 10 g/L, 5 g/L, 1 g/L.

3. Results and discussion

3.1. Bio-prospecting for methyl ketone synthases

E. coli FadM had significantly lower activity on C_8-C_{12} saturated acyl-CoAs than C_{14}-C_{16} acyl-CoAs in *in vitro* kinetic studies using saturated, unsaturated, and hydroxylated acyl-CoA substrates, (Nie et al., 2008). In our study, we targeted production of medium-chain methyl-ketones and therefore started with a bioprospecting study to identify FadM homologs with high activity towards substrates (acyl-CoA or acyl-ACP) with twelve or less carbons. We conducted a homology search with the Basic Local Alignment Search Tool to identify candidate protein sequences. The search generated a wide range of biological diversity that we sorted using the Enzyme Similarity Tool. We selected fifteen FadM homologs which had a protein sequence similarity range of 30-95% based on a pairwise comparison of each thioesterase, shown in **Figure S1A**. We were particularly interested in homologs from *Salmonella enterica* (*Se*FadM) and *Pseudomonas aeruginosa* (*Pa*FadM) because these species were known to have strong β-oxidation activities (Chakrabarty et al., 1973; Iram and Cronan, 2006) and have been sources of active enzymes used in prior studies (Mehrer et al., 2018). *Mycobacterium tuberculosis* possessed several type III thioesterases that have been previously shown activities towards acyl-CoAs (Wang et al., 2007) and five different homologs (*Mt*1-*Mt*5 FadM) were found that shares 26-58% similarities to the ^{Ec}FadM **Figure S1B**.

The activity of the FadM homologs was assayed *in vivo* by feeding fatty acids of varied chain length to *E. coli ΔfadAIR* + pTRC99a-FadD6-"FadM", and monitoring fatty acid

consumption and methyl ketone production, **Figure 2**. ^{Mt}FadD6 was overexpressed to increase the acyl-CoA synthetase activity required to activate the exogenous fatty acids fed to cells. ^{Mt}FadD6 has been shown to act on medium-chain free fatty acids with greater activity than native FadD from *E. coli* (Youngquist et al., 2013, Herneandez-Lozada et al., Under Review). The *ΔfadR* deletion was included to deregulate expression of FadE and FadB, which are responsible for the conversion of saturated acyl-CoA to the corresponding 3-ketoacyl-CoA. The *ΔfadAI* deletions were included to block the thiolase reaction that would otherwise lead to the shortening of the 3-ketoacyl-CoA. Given the metabolic engineering strategy used, any fatty acid consumption would be coupled to production of the corresponding methyl ketone. In **Figure 2**, we report both the fatty acid consumption rate (timecourses available in **Figure S2**) and the measured titer of methyl ketones because many medium-chain methyl ketones are volatile and lost from the headspace of the flask. In general, the trend of fatty acid consumption rate between enzyme variants tracked with the trend of methyl ketone production (**Figure 2**). We found that *Providencia sneebia* FadM showed the highest activities toward medium-chain substrates and produced ~50 mg/L 2-heptanone, ~43 mg/L 2-nonanone, and 50 mg/L 2-undecanone. In general, the *P. sneebia* FadM showed high activity against each chain length tested, within error of the best enzymes producing pentadecanone and heptadecanone (**Figure 2**).

A. Schematic of Bioprospecting Assay

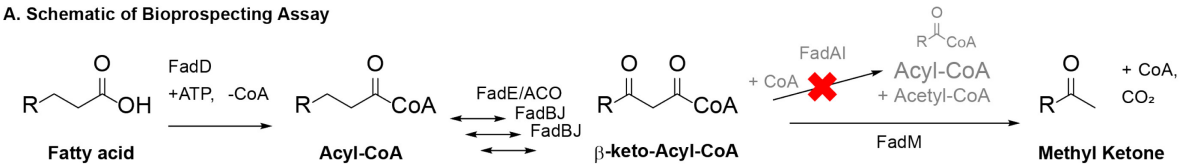

B. Evaluation of FadM Homologs

	C7 MK Titer (mg/L)	C8 FFA Consump. (mg/L/h)	C9 MK Titer (mg/L)	C10 FFA Consump. (mg/L/h)	C11 MK Titer (mg/L)	C12 FFA Consump. (mg/L/h)	C13 MK Titer (mg/L)	C14 FFA Consump. (mg/L/h)	C15 MK Titer (mg/L)	C16 FFA Consump. (mg/L/h)	
Control	0.4 ± 0.1	14.5 ± 2.7	2.3 ± 0.1	2.1 ± 0.4	0.5 ± 0.0	2.3 ± 0.2	7.4 ± 1.2	6.8 ± 1.5	1.2 ± 0.8	3.5 ± 0.2	Control
SeFadM	4.7 ± 0.7	18.1 ± 3.5	10.9 ± 0.6	3.9 ± 0.4	16.0 ± 2.3	9.7 ± 0.6	22.3 ± 2.7	17.5 ± 0.9	36.2 ± 4.7	6.0 ± 1.0	SeFadM
NgFadM	4.9 ± 0.5	5.2 ± 3.4	8.1 ± 0.4	6.0 ± 0.3	22.8 ± 1.5	13.7 ± 0.9	18.5 ± 2.5	15.4 ± 3.8	22.0 ± 10.1	7.6 ± 1.0	NgFadM
MtFadM5	5.3 ± 0.3	5.2 ± 2.9	10.0 ± 0.4	5.3 ± 0.2	27.7 ± 0.1	12.9 ± 1.0	22.9 ± 1.7	17.4 ± 0.5	35.1 ± 1.6	6.2 ± 1.8	MtFadM5
MuFadM	5.6 ± 0.0	10.2 ± 1.3	6.5 ± 0.7	6.5 ± 0.4	17.7 ± 0.0	10.9 ± 0.5	21.9 ± 2.1	14.4 ± 1.2	17.1 ± 1.0	7.0 ± 0.4	MuFadM
PaFadM	5.9 ± 0.1	2.5 ± 2.1	2.3 ± 0.1	2.1 ± 0.4	13.9 ± 2.3	7.0 ± 0.5	18.1 ± 0.1	9.1 ± 2.7	6.0 ± 4.2	5.7 ± 0.1	PaFadM
BaFadM	7.9 ± 0.4	17.2 ± 2.0	6.3 ± 0.4	16.4 ± 0.5	21.9 ± 2.1	13.2 ± 0.2	32.2 ± 7.7	14.5 ± 0.7	31.8 ± 4.2	7.5 ± 0.8	BaFadM
MtFadM1	8.0 ± 0.3	26.9 ± 7.8	14.4 ± 1.1	26.2 ± 0.6	37.9 ± 9.1	15.0 ± 0.2	29.8 ± 3.2	17.0 ± 1.7	28.1 ± 4.7	9.1 ± 1.0	MtFadM1
MtFadM4	10.0 ± 0.2	25.8 ± 2.6	12.0 ± 0.2	25.8 ± 0.7	31.6 ± 1.2	14.7 ± 0.4	29.8 ± 4.2	16.3 ± 2.6	28.4 ± 10.6	7.9 ± 3.5	MtFadM4
MtFadM3	11.4 ± 0.0	26.2 ± 9.3	9.0 ± 0.6	26.9 ± 0.6	13.9 ± 1.4	6.1 ± 0.6	19.8 ± 4.0	4.3 ± 0.5	32.8 ± 2.4	6.2 ± 0.2	MtFadM3
MtFadM2	11.8 ± 0.3	41.9 ± 3.6	18.8 ± 0.8	28.9 ± 0.2	43.5 ± 5.0	14.4 ± 0.9	33.2 ± 1.2	15.2 ± 2.4	35.4 ± 1.5	8.2 ± 0.8	MtFadM2
SoFadM	13.9 ± 0.1	104.9 ± 17.1	25.3 ± 0.8	77.4 ± 1.2	32.0 ± 1.0	15.6 ± 1.4	39.0 ± 6.6	15.4 ± 0.5	40.2 ± 12.0	8.3 ± 2.9	SoFadM
BbFadM	15.5 ± 0.5	89.2 ± 4.8	25.2 ± 1.2	64.2 ± 0.4	20.2 ± 4.4	8.4 ± 0.3	29.1 ± 6.4	13.4 ± 0.3	34.2 ± 1.5	8.3 ± 1.9	BbFadM
EclFadM	24.7 ± 0.5	102.5 ± 7.6	29.1 ± 0.2	71.7 ± 1.0	41.6 ± 5.2	14.8 ± 0.3	39.9 ± 0.3	17.2 ± 0.8	38.7 ± 0.5	11.6 ± 2.7	EclFadM
CtFadM	26.4 ± 0.7	115.6 ± 3.1	20.5 ± 0.4	32.9 ± 1.1	20.6 ± 3.8	12.3 ± 2.1	27.8 ± 7.3	9.6 ± 1.5	38.6 ± 8.4	11.0 ± 2.0	CtFadM
EcFadM	33.3 ± 0.2	105.7 ± 0.8	30.3 ± 1.0	58.9 ± 0.8	40.0 ± 1.4	14.5 ± 1.0	44.6 ± 9.7	17.1 ± 0.0	45.3 ± 11.6	9.5 ± 1.2	EcFadM
PsFadM	50.0 ± 0.2	142.9 ± 7.0	43.3 ± 1.0	137.0 ± 0.2	49.5 ± 1.3	13.6 ± 0.3	39.0 ± 3.4	15.4 ± 3.5	36.9 ± 0.7	7.4 ± 0.8	PsFadM

Figure 2 (A) Scheme describing bioconversion of free fatty acids to methyl ketones. FadM variants were expressed from pTRC99a-"FadM"-FadD6 in strain *E. coli* ΔRAI. **(B)** FadM activity was tested by feeding even chain-length saturated fatty acids to the culture and measuring the concentration of methyl ketones and free fatty acids over 24 hours. The MK titer is listed in the left column of each pair. A fatty acid consumption rate was calculated from the timecourses presented in **Figure S2**. Cells were fed 1 g/L octanoic acid, 1 g/L decanoic acid 200 mg/L dodecanoic acid, 100 mg/L tetradecanoic acid, or 100 mg/L hexadecanoic acid. The listed error is the standard deviation of measurements taken from triplicate flasks.

3.2. Metabolic engineering to improve 2-heptanone production

After identifying promising FadM variants, we next developed a strain to produce 2-heptanone utilizing the modified β-oxidation pathway outlined in **Figure 3A** and a previously characterized acyl-ACP thioesterase with strong activity towards octanoyl-ACP. The base strain for this study was *E. coli* NHL17 (MG1655 ΔaraBAD ΔfadD::trc-CpFatB1*) which has been shown to produce up to 1.7 g/L of octanoic acid (Hernández Lozada et al., 2018). To improve the flux towards 2-heptanone, *fadA*, *fadI*, and *fadR* were deleted from NHL17 to generate the strain

TRS12. These deletions were included for the same reasons described above - blocking thiolase reactions and upregulating FadE and FadB. The FadM activity in TRS12 solely came from the chromosomal expression of the native ^{Ec}FadM. This strain generated low titers, < 1 mg/L, of 2-heptanone (data not shown). To improve production further, we overexpressed ^{Ec}FadM from the high copy plasmid, pTRC99a-FadD6-*Ec*FadM. This strain generated a titer of 2.4 mg/L of 2-heptanone (**Figure 3**). In order to increase the flux from acyl-CoA to enoyl-CoA we overexpressed ^{Ec}FadE. This modification led to a ten-fold increase in 2-heptanone concentration, to a final titer of 21.9 mg/L (**Figure 3**). We next replaced ^{Ec}FadM with ^{Ps}FadM, the most active variant from our bioprospecting study, to make the expression plasmid, pTRC99a-FadD6-*Ps*FadM. When co-expressed with ^{Ec}FadE, the strain generated a final titer of 78.4 mg/L 2-heptanone (**Figure 3**). Lastly, ^{Ec}FadE was replaced with the acyl-CoA oxidase from *M. luteus* (Goh et al. 2012), and was co-expressed from the pACYC-Mlut_11700 plasmid alongside pTRC99a-FadD6-*Ps*FadM. Replacing the membrane protein ^{Ec}FadE with the soluble heterologous acyl-CoA oxidase increased the 2-heptanone titer to 215.2 mg/L (**Figure 3**) with 97% selectivity. We suspect that this titer is underestimated, because when we incubated a defined 5 g/L 2-heptanone/water solution with 10% dodecane (v/v) in the same shake flasks, we observed that ~70% of the 2-heptanone was lost (**Figure S3A**) after 24 hours.

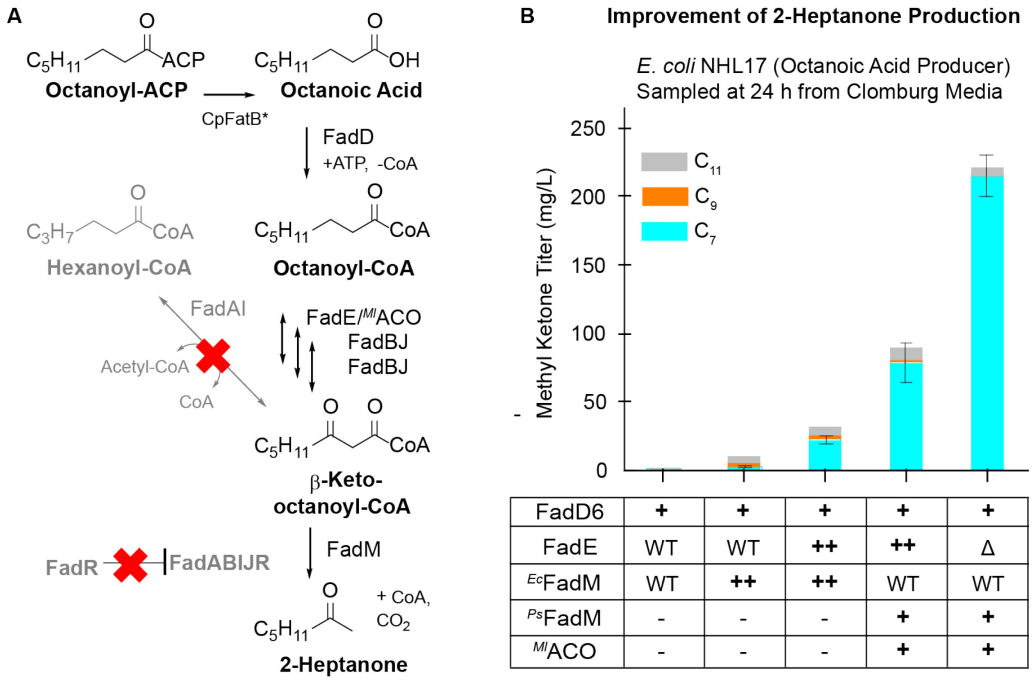

FadD6	+	+	+	+	+
FadE	WT	WT	++	++	Δ
EcFadM	WT	++	++	WT	WT
PsFadM	-	-	-	+	+
MlACO	-	-	-	+	+

Figure 3 Scheme of genetic design to improve 2-heptanone titer (A), genetic modifications based on strain NHL17 were marked in red, resulted in strain TRS12 (NHL17, Δ*fadAEIR*) expressing pTRC99a-fadD6-fadM and pACYC-Mlut_11700. Stepwise improvement of 2-heptanone production from engineered *E. coli* NHL17 strains from 20 g/L glycerol in Clomburg medium (B). "WT" refers to native expression of the gene, "+" represents an exogenous gene is overexpressed in a plasmid, "++" represents an endogenous gene has a chromosomal copy and was overexpressed in a plasmid, "-" represents a heterologous gene that was not added, Δ represents a native gene that was removed from the chromosome.

3.3. Coupling bioreactor with condenser to reduce 2-heptanone loss

To benchmark methyl ketone production, we conducted fed-batch cultivations by periodically feeding glycerol boluses to cells grown in a stirred bioreactor. We applied two strategies to reduce the loss of 2-heptanone in the off-gas: adding 20% dodecane to the culture (**Figure S3A**) and coupling a condenser to the bioreactor to harvest vaporized 2-heptanone (**Figure S4**). After 72 h of induced cultivation, cells consumed 111.5 g/L of glycerol, reached a biomass density of OD_{600} ~40, and produced 3.34 g/L methyl ketone titer (**Figure 4A**). When a condenser was added to the off-gas line, we observed a similar trend of glycerol consumption, biomass formation and methyl ketone production with modestly increased titers. After 72 h of induced cultivation, cells consumed

126 g/L glycerol, reached a biomass density of OD_{600} ~50, produced 4.4 g/L methyl ketone at the maximum titer (**Figure 4B**). At longer times, the titer of methyl ketones decreased, likely due to the rate of evaporation exceeding the rate of generation, which one would expect to be low as the carbon source, glycerol, is exhausted. After 96 hours, we observed a small amount (~ 25 mL of 2.3 g/L) of a MK containing solution in the condensed phase, representing ~5% of total MK titer **(Figure 4C)**. We suspect that we may either be failing to provide sufficient cooling duty or we may be stripping MK from the condensed phase with our current design (**Figure S4**). Further work will be needed to identify condenser configurations or other capturing strategies to recover volatile MK from culture. The volatility and ability to be stripped from culture may be advantageous when scaling up the process.

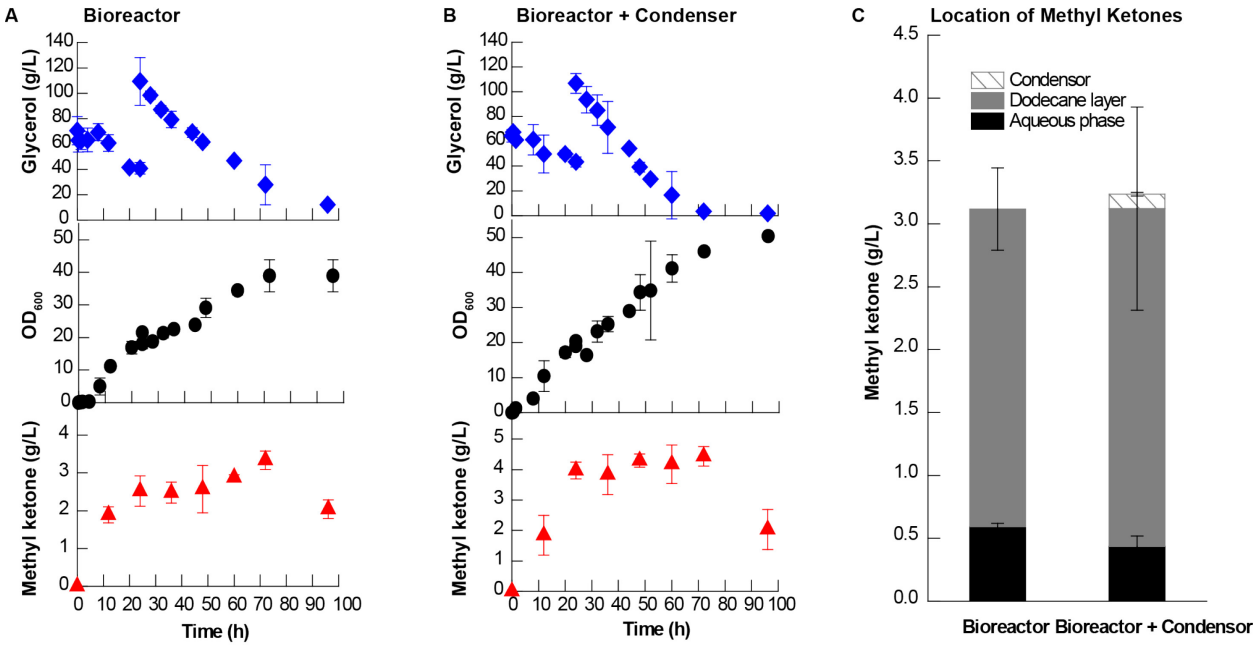

Figure 4 Time course of concentration of glycerol, OD_{600} and total methyl ketone in fed-batch fermentation from bioreactor (A) and bioreactor coupling a condenser (B) using *E. coli* TRS12 strain harbors pTRC99a-FadD6-*Ps*FadM and pACYC-Mlut_11700 plasmids. (C) Evaluation of methyl ketone concentration from samples in dodecane layer, aqueous phase and condenser after 96 h fermentation.

3.4. Metabolic engineering to improve 2-nonanone production

Our initial experiments suggested that the oxidation of saturated acyl-CoAs was a limiting factor in converting free fatty acids to methyl-ketones (i.e. acyl-CoA oxidase improved production). Therefore, we considered an alternative pathway in which oxidation was replaced by thiolase-mediated extension of the saturated acyl-CoA to a β-ketoacyl-CoA with two extra carbons. This idea is modeled off of the reverse β-oxidation pathway that has been shown to produce long chain acyl-CoAs in *E. coli* fermentations (Dellomonaco et al., 2011; Mehrer et al., 2018). The thiolase route avoids the need to generate NADH when cells are actively metabolizing glycerol and already have a highly reduced ratio of NADH/NAD+. To test this approach, we cloned a family of seven thiolase enzymes into a pACYC vector and coexpressed each with pTRC99a-FadD6-*Ps*fadM in *E. coli* Δ*fadABIJR*. The activity of the ^{Ec}FadA homologs was assayed *in vivo* by feeding 0.5 g/L octanoic acid to *E. coli ΔfadABIJR* + pTRC99a-FadD6-PsFadM + pACYC-"FadA", and monitoring octanoic acid consumption and 2-nonanone production, **Figure 5A**. In general, all seven thiolase enzymes conferred the ability to consume octanoic acid and produce 2-nonanone (**Figure 5B and S5A**). In terms of ranking, we found strains expressing ^{Re}BktB and ^{Se}FadA exhibited the highest consumption rates (over 80% octanoic acid consumed within 18 h) and 2-nonanone titers (~280 mg/L) (**Figure 5B and S5B).**

Next, we evaluated 2-nonanone production from glycerol in the background strain *ΔfadAIR* pTRC99a-FadD6-*Ps*FadM + pACYC-*Re*BktB + pBTRCK-*CpFatB1**. After 24 h in a batch shake flask culture, strains produced ~1.15 g/L 2-nonanone representing 75% of total methyl ketones from the 45 g/L glycerol fed (**Figure 5C** and **5D**). We also suspect that the titer is underestimated, because when we incubated a defined 3.3 g/L 2-nonanone/water solution in the same shake flasks, we observed that 90% of the 2-nonanone was lost within 24 h (**Figure S3A**).

To benchmark 2-nonanone production, we conducted fed-batch cultivations by bolus feeding glycerol to cells grown in a stirred bioreactor. In order to reduce the loss of 2-nonanone in the off-gas, we applied the two strategies: adding 20% dodecane to the culture and coupling a condenser to the bioreactor to harvest vaporized 2-nonanone (**Figure S4**). After 72 h post-induction, cells consumed 107.1 g/L of glycerol, reached a biomass density of OD600 ~52, and produced a 3.0 g/L methyl ketone titer (**Figure 5E**). When a condenser was applied to the off-gas line, we observed a similar trend of glycerol consumption, biomass formation and methyl ketone production (data not shown). After 96 h post-induction, we found ~23 mL liquid containing ~120 mg/L methyl ketones collected in the condenser, representing less than 1% total MK. Overall, our results showed the thiolase-mediated condensation route is capable of producing 2-nonanone, but further optimization is needed to avoid the loss of octanoic acid intermediates from the cell (**Figure S5C**).

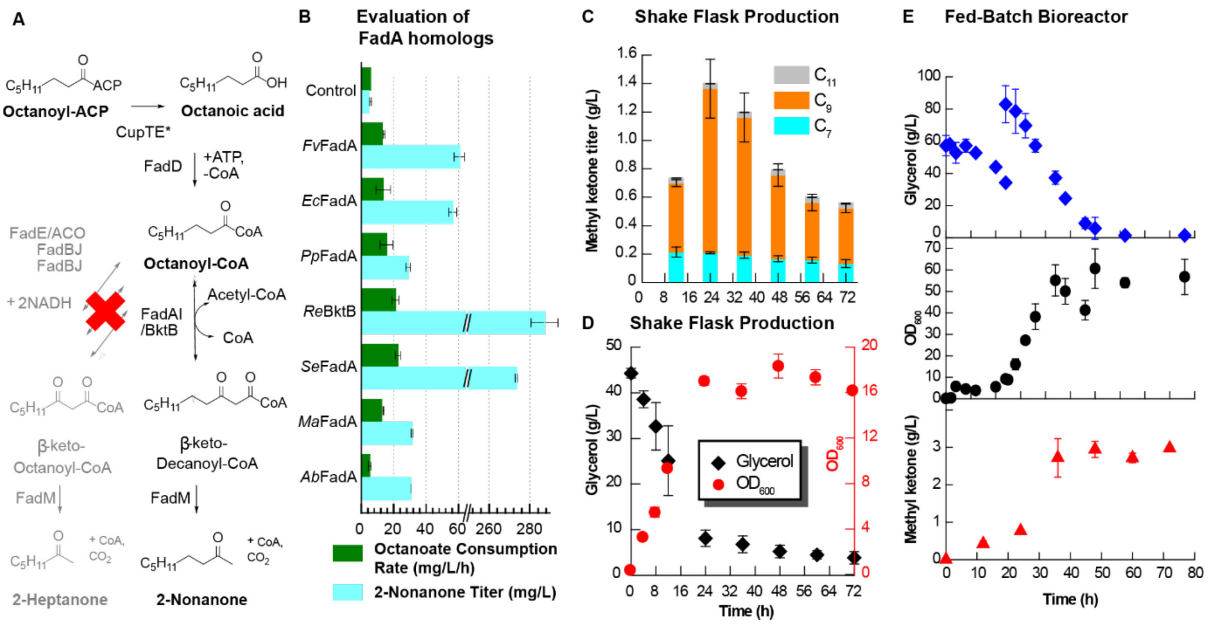

Figure 5 (A) Metabolic pathway for synthesis of 2-nonanone. Strain *E. coli* Δ*fadRABIJ* expressing pACYC-"fadA" + pTRC99a-FadD6-*Ps*FadM + pBTRCK-*Cp*FatB1* was used for demonstrating 2-nonanone synthesis. Impact of acyl-CoA thiolase homologs on rates of octanoic consumption (B) and 2-nonanone production (C) were evaluated by *in vivo* feeding 500 mg/L octanoic acid to the culture. The negative control is the strain harbored pACYC empty plasmid. Shake flask batch

fermentation for 2-nonanone production was conducted by grown *E. coli ΔfadABIJR* strain that harbors pACYC-*Re*BktB + pTRC99a-FadD6-*Ps*FadM + pBTRCK-*Cp*FatB1* plasmids in Clomburg medium containing 45 g/L glycerol. Time course of methyl ketone titer (C), glycerol titer and OD600 (D) were monitored every 4 - 12 hrs. (E) Time course of glycerol titer, OD_{600} and methyl ketone titer in fed-batch fermentation in a bioreactor using the optimized strain. All error bars represent standard deviations calculated from at least three biological replicates.

3.5. Metabolic engineering to improve 2-undecanone production

The *Umbellularia californica* acyl-ACP thioesterase BTE has high activity towards C_{12} acyl-ACPs. BTE has been used in metabolic pathways to produce dodecanoate, 1-dodecanol, and polyhydroxydodecanoate, etc (Agnew et al., 2012; Lennen et al., 2010; Youngquist et al., 2013). Therefore, we used BTE to generate dodecanoate as an intermediate to enzymatically produce 2-undecanone. To test this approach, we chose a base strain TY34 (*ΔfadE::trcBTE ΔfadAB::trcBTE ΔackApta::trcBTEΦ(PTrc-fadD*) from Youngquist et al., 2013, in which 1-dodecanol was produced in titers over 1 g/L. To this strain, we introduced Mlut_11700, ^{Ps}FadM, and increased expression of ^{Ec}FadD. Mlut_11700 was selected for its higher activity in catalyzing the dehydrogenation of acyl-CoA to 2-enoyl-CoA. ^{Ps}FadM was selected from the 15 homologs tested in **Figure 2** for its strong activity towards twelve carbon substrates. We selected ^{Ec}FadD instead of ^{Mt}FadD6 because ^{Ec}FadD was previously shown higher activities converting dodecanoate to dodecanoyl-CoA (Youngquist et al., 2013). We chose to overexpress a FadB homolog because the endogenous ^{Ec}*fadAB* operon in TY34 strain was replaced by one copy of BTE.

In prior work, we observed that the source of the FadAB complex affected the product profile from reverse β-oxidation cycles activities (Mehrer et al., 2018), indicating that there may be chain length preferences. We chose six FadB homologs from which have previously shown functional FadAB complexes when testing reversed β-oxidation pathways (Mehrer et al., 2018). We evaluated each by comparing 2-undecanone titers in TY34 strains harboring three plasmids:

pACYC-"FadB", pBTRCK-Mlu_11700, and pTRC99a-*Ps*FadM (**Figure 6A)**. While control strains harboring a pACYC empty vector could not produce 2-undecanone, strains expressing each FadB homolog showed substantial quantities of 2-undecanone **(Figure 6B)**. The strain harboring FadB from *Pseudomonas putida* generated the highest titer (350 mg/L) of methyl ketones and the highest specificity (58%) towards 2-undecanone. This result is not surprising considering *P. putida* naturally accumulates medium-chain length polyhydroxyalkanoate (PHA) and likely maintains a relatively higher C_8-C_{12} activity to provide sufficient 3-hydroxylacyl-CoA pools, the most common substrates for PHA synthases PhaC1/C2 (Hoffmann and Rehm, 2004, 2005).

Next, we evaluated 2-undecanone synthesis in a time course experiment by growing strains in a shake flask in batch mode. We monitored cell growth, glycerol consumption, methyl ketone production, and fatty acid intermediates. As can be seen in **Figure 6C** and **6D**, 25 g/L glycerol was depleted after 36 h. Cell growth reached a plateau after ~12 h, and the highest 2-undecanone concentration 335 mg/L was observed at ~48 h. The 2-undecanone titer represented ~62% of the total amount of methyl ketones. Overall, these data showed that we have successfully designed and optimized strains and metabolic enzymes to improve 2-undecanone production. Interestingly, the titers of 2-undecanone were significantly lower than those observed for 2-heptanone and 2-nonanone. This may be due to the difference in activity between the CpFatB1* and BTE thioesterases; residual levels of dodecanoic acid and tetradecanoic acid were substantially lower than residual octanoic acid (**Figure S6**).

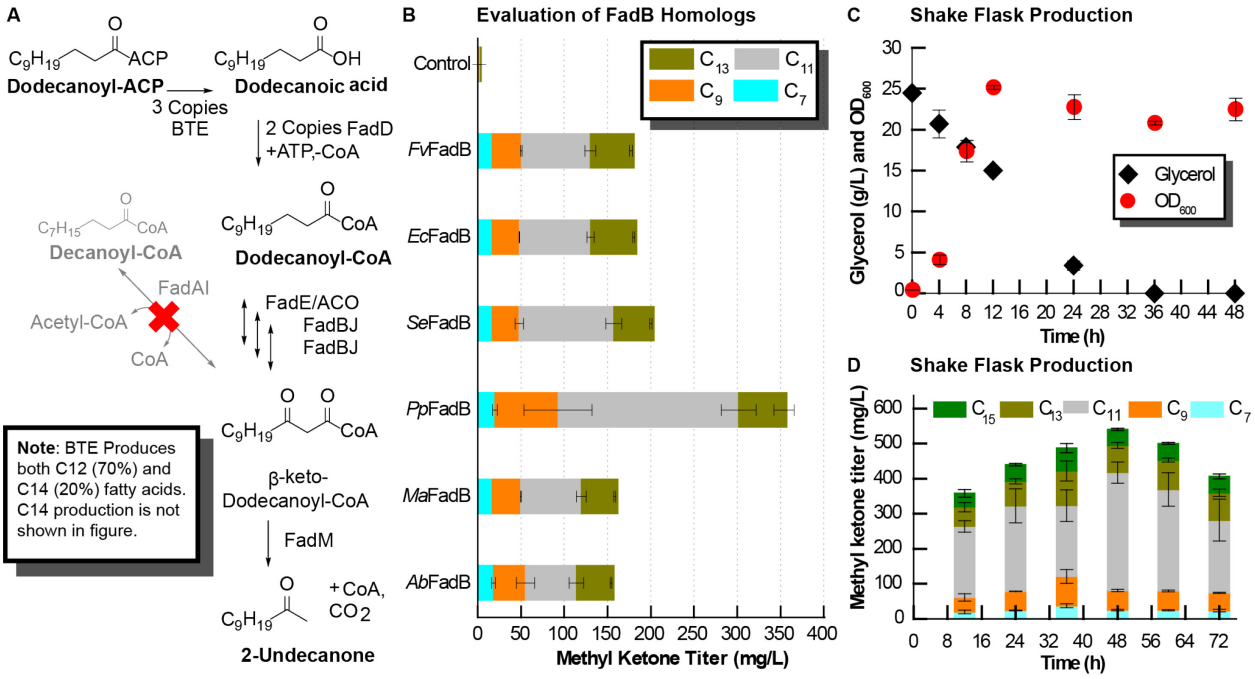

Figure 6 (A) Designed a metabolic pathway for production of 2-undecanone. (B) Comparison of bi-functional 3-hydroxyacyl-CoA dehydratase. *E. coli* TY34 strain harbors pACYC-FadB + pTRC99a-*Ps*fadM + pBTRCK-Mlut_11700 plasmids were grown in Clomburg medium containing 20 g/L glycerol for 24 h. (C) Time course of glycerol consumption and biomass formation, and (D) methyl ketone production by *E. coli* TY34 strain harbors pACYC-*Pp*FadB + pTRC99a-*Ps*fadM plasmids were grown in Clomburg medium containing 25 g/L glycerol for 72 h.

Table 2. Summary of reported titer, yield and rate of methyl ketone production by microorganisms.

Product	Titers (g/L)	Yield (g/g)	Rate (g/L/h)	Cultivation Strategies	Species	References
2-heptanone	4.4	0.035 g/g consumed glycerol	0.061	bioreactor, fed-batch	*E. coli*	this study
2-nonanone	3.0	0.028 g/g consumed glycerol	0.042	bioreactor, fed-batch	*E. coli*	this study
2-undecanone	0.34	0.014 g/g consumed glycerol	0.007	shake flask, batch	*E. coli*	this study
C_{11}-C_{15} MK	5.4	~0.05 g/g consumed glucose	0.05	bioreactor, fed-batch	*E. coli*	Goh et al., 2018
2-pentanone	0.24	0.024 g/g consumed glucose	0.0033	shake flask, batch	*E. coli*	Lan et al., 2013
C_{13}-C_{23} MK	0.31	0.0074 g/g fed glucose	0.00155	bioreactor, fed-batch	*Y. lipolytica*	Hanko et al., 2018
C_{11}-C_{15} MK	10 [a]	NR	NR	shake flask, batch	*S. cerevisiae*	Zhu et al., 2017
2-butanone 2-heptanone	0.24	0.0028 g/g fed hydrolysate	0.0011	bioreactor, batch	*S. albus*	Yuzawa et al., 2018
C_{13}-C_{15} MK	1.1	0.169 g/g fed glucose	0.023	shake flask, batch	*P. putida*	Dong et al., 2019
C_{13}-C_{15} MK	0.18	NR	0.0015	bioreactor, batch	*R. eutropha*	Muller et al., 2013

NR = Not reported

[a] μg/DCW

[b] Yield is calculated as either g/g fed carbon source or g/g consumed carbon source, where former is quantified by dividing the reported titer (g/L) over the initial carbon concentration and the latter is directly reported in the original papers.

4. Conclusion

In this work, we demonstrated metabolic engineering strategies for selective synthesis of 2-heptanone, 2-nonanone and 2-undecanone in *E. coli*. Through bioprospecting, we identified a FadM variant from *Providencia sneebia* that demonstrated higher activity on medium-chain substrates. When co-expressed with selective thioesterases it was capable of producing three different chain length MK products. In each case, the MK product profile was consistent with the selectivity of the thioesterase used. We demonstrated a novel thiolase-condensation route for converting acyl-CoAs to β-ketoacyl-CoA, the FadM substrate. When co-expressed with the CpFatB1*, a strain produced 2-nonanone with a titer up to 3.0 g/L; the highest reported titer to date (Table 2). Interestingly, this strain also excreted substantial amounts of octanoic acid, indicating that further optimization could further improve titers. In each of our studies, we observed substantial product loss due to evaporation and stripping. We coupled a rudimentary, water-cooling condenser to a bioreactor and found that it helped to increase titers over the timecourse, but failed to prevent product loss after metabolism ceased. While the evaporative loss is a challenge that leads to underestimation of product titers, it may be an advantage when scaling up MK production.

5. Author contributions

Q.Y., T.R.S., N.J.H., and B.F.P. conceived the study. Q.Y. and T.R.S performed the experiments and analyzed the data. Q.Y., T.R.S., W.T.C. and B.F.P. wrote the manuscript. W.T.C. and M.A.J. contributed to the condenser and bioreactor work. C.J.B. and X.C. contributed to plasmid construction.

6. Declaration of competing interest

No conflict of interest was declared for this study.

7. Acknowledgements

This work was funded by the National Science Foundation (CBET-1703504) and the DOE Center for Advanced Bioenergy and Bioproducts Innovation (U.S. Department of Energy, Office of Science, Office of Biological and Environmental Research under Award Number DE-SC0018420). Any opinions, findings, and conclusions or recommendations expressed in this publication are those of the author(s) and do not necessarily reflect the views of the U.S. Department of Energy or the National Science Foundation. N.J.H.-L. is the recipient of a NIH Chemistry-Biology Interface Training Program fellowship (No. T32 GM008505) and a Graduate Engineering Research Scholars fellowship from the UW−Madison College of Engineering.

References

Agnew, D.E., Stevermer, A.K., Youngquist, J.T., Pfleger, B.F., 2012. Engineering *Escherichia coli* for production of C12–C14 polyhydroxyalkanoate from glucose. Metab. Eng. 14, 705–713. https://doi.org/10.1016/j.ymben.2012.08.003

Cantu, D.C., Chen, Y., Lemons, M.L., Reilly, P.J., 2011. ThYme: a database for thioester-active enzymes. Nucleic Acids Res. 39, D342–D346. https://doi.org/10.1093/nar/gkq1072

Chakrabarty, A.M., Chou, G., Gunsalus, I.C., 1973. Genetic Regulation of Octane Dissimilation Plasmid in *Pseudomonas*. Proc. Natl. Acad. Sci. 70, 1137–1140. https://doi.org/10.1073/pnas.70.4.1137

Collins, Y.F., McSweeney, P.L.H., Wilkinson, M.G., 2003. Lipolysis and free fatty acid catabolism in cheese: a review of current knowledge. Int. Dairy J. 13, 841–866. https://doi.org/10.1016/S0958-6946(03)00109-2

Clomburg, J.M., Vick, J.E., Blankschien, M.D., Rodríguez-Moyá, M., Gonzalez, R., 2012. A Synthetic Biology Approach to Engineer a Functional Reversal of the β-Oxidation Cycle. ACS Synth. Biol. 1, 541–554. https://doi.org/10.1021/sb3000782

Dellomonaco, C., Clomburg, J.M., Miller, E.N., Gonzalez, R., 2011. Engineered reversal of the β-oxidation cycle for the synthesis of fuels and chemicals. Nature 476, 355–359. https://doi.org/10.1038/nature10333

Dong, J., Chen, Y., Benites, V.T., Baidoo, E.E.K., Petzold, C.J., Beller, H.R., Eudes, A., Scheller, H. V., Adams, P.D., Mukhopadhyay, A., Simmons, B.A., Singer, S.W., 2019. Methyl ketone

production by *Pseudomonas putida* is enhanced by plant-derived amino acids. Biotechnol. Bioeng. 116, 1909–1922. https://doi.org/10.1002/bit.26995

Dyrløv Bendtsen, J., Nielsen, H., von Heijne, G., Brunak, S., 2004. Improved Prediction of Signal Peptides: SignalP 3.0. J. Mol. Biol. 340, 783–795. https://doi.org/10.1016/j.jmb.2004.05.028

Forney, F., Markovetz, A., 1971. The biology of methyl ketones. J. Lipid Res. 12, 383–395.

Frias, J.A., Richman, J.E., Erickson, J.S., Wackett, L.P., 2011. Purification and Characterization of OleA from Xanthomonas campestris and Demonstration of a Non-decarboxylative Claisen Condensation Reaction. J. Biol. Chem. 286, 10930–10938. https://doi.org/10.1074/jbc.M110.216127

Harrison, K.W., Harvey, B.G., 2018. High cetane renewable diesel fuels prepared from bio-based methyl ketones and diols. Sustain. Energy Fuels 2, 367–371. https://doi.org/10.1039/C7SE00415J

Hoekman, S.K., Broch, A., Robbins, C., Ceniceros, E., Natarajan, M., 2012. Review of biodiesel composition, properties, and specifications. Renew. Sustain. Energy Rev. 16, 143–169. https://doi.org/10.1016/j.rser.2011.07.143

Gibson, D.G., Young, L., Chuang, R.-Y., Venter, J.C., Hutchison, C.A., Smith, H.O., 2009. Enzymatic assembly of DNA molecules up to several hundred kilobases. Nat. Methods 6, 343–345. https://doi.org/10.1038/nmeth.1318

Goh, E.-B., Baidoo, E.E.K., Keasling, J.D., Beller, H.R., 2012. Engineering of Bacterial Methyl Ketone Synthesis for Biofuels. Appl. Environ. Microbiol. 78, 70–80. https://doi.org/10.1128/AEM.06785-11

Goh, E.-B., Baidoo, E.E.K., Burd, H., Lee, T.S., Keasling, J.D., Beller, H.R., 2014. Substantial improvements in methyl ketone production in *E. coli* and insights on the pathway from *in vitro* studies. Metab. Eng. 26, 67–76. https://doi.org/10.1016/j.ymben.2014.09.003

Goh, E.-B., Chen, Y., Petzold, C.J., Keasling, J.D., Beller, H.R., 2018. Improving methyl ketone production in *Escherichia coli* by heterologous expression of NADH-dependent FabG. Biotechnol. Bioeng. 115, 1161–1172. https://doi.org/10.1002/bit.26558

Grisewood, M.J., Hernández-Lozada, N.J., Thoden, J.B., Gifford, N.P., Mendez-Perez, D., Schoenberger, H.A., Allan, M.F., Floy, M.E., Lai, R.-Y., Holden, H.M., Pfleger, B.F., Maranas, C.D., 2017. Computational Redesign of Acyl-ACP Thioesterase with Improved Selectivity toward Medium-Chain-Length Fatty Acids. ACS Catal. 7, 3837–3849. https://doi.org/10.1021/acscatal.7b00408

Hanko, E.K.R., Denby, C.M., Sànchez i Nogué, V., Lin, W., Ramirez, K.J., Singer, C.A., Beckham, G.T., Keasling, J.D., 2018. Engineering β-oxidation in *Yarrowia lipolytica* for methyl ketone production. Metab. Eng. 48, 52–62. https://doi.org/10.1016/j.ymben.2018.05.018

Harrison, K.W., Harvey, B.G., 2018. High cetane renewable diesel fuels prepared from bio-based methyl ketones and diols. Sustain. Energy Fuels 2, 367–371. https://doi.org/10.1039/C7SE00415J

Hernández Lozada, N.J., Lai, R.-Y., Simmons, T.R., Thomas, K.A., Chowdhury, R., Maranas, C.D., Pfleger, B.F., 2018. Highly Active C 8 -Acyl-ACP Thioesterase Variant Isolated by a Synthetic Selection Strategy. ACS Synth. Biol. 7, 2205–2215. https://doi.org/10.1021/acssynbio.8b00215

Hernández Lozada, N.J., Simmons, T.R., Xu, K., Jindra, M.A., Pfleger, B.F., 2020. Production of

1-octanol in *Escherichia coli* by a high flux thioesterase route. doi: Under review.

Hoffmann, N., Rehm, B.H.., 2004. Regulation of polyhydroxyalkanoate biosynthesis in *Pseudomonas putida* and *Pseudomonas aeruginosa*. FEMS Microbiol. Lett. 237, 1–7. https://doi.org/10.1111/j.1574-6968.2004.tb09671.x

Hoffmann, N., Rehm, B.H.A., 2005. Nitrogen-dependent regulation of medium-chain length polyhydroxyalkanoate biosynthesis genes in pseudomonads. Biotechnol. Lett. 27, 279–282. https://doi.org/10.1007/s10529-004-8353-8

Iram, S.H., Cronan, J.E., 2006. The β-Oxidation Systems of *Escherichia coli* and *Salmonella enterica* Are Not Functionally Equivalent. J. Bacteriol. 188, 599–608. https://doi.org/10.1128/JB.188.2.599-608.2006

Kennedy, G.G., 2003. Tomato, pests, parasitoids, and predators: tritrophic interactions involving the genus Lycopersicon. Annu. Rev. Entomol. 48, 51–72. https://doi.org/10.1146/annurev.ento.48.091801.112733

Kornberg, A., Ochoa, S., Mehler, A.H., 1948. Spectrophotometric studies on the decarboxylation of β-keto acids. J. Biol. Chem. 174, 159.

Kim, E.-J., Son, H.F., Kim, S., Ahn, J.-W., Kim, K.-J., 2014. Crystal structure and biochemical characterization of beta-keto thiolase B from polyhydroxyalkanoate-producing bacterium *Ralstonia eutropha* H16. Biochem. Biophys. Res. Commun. 444, 365–369. https://doi.org/10.1016/j.bbrc.2014.01.055

Lan, E.I., Dekishima, Y., Chuang, D.S., Liao, J.C., 2013. Metabolic engineering of 2-pentanone

synthesis in *Escherichia coli*. AIChE J. 59, 3167–3175. https://doi.org/10.1002/aic.14086

Lennen, R.M., Braden, D.J., West, R.M., Dumesic, J.A., Pfleger, B.F., 2010. A process for microbial hydrocarbon synthesis: Overproduction of fatty acids in *Escherichia coli* and catalytic conversion to alkanes. Biotechnol. Bioeng. 106, 193–202. https://doi.org/10.1002/bit.22660

Lian, J., Zhao, H., 2015. Reversal of the β-Oxidation Cycle in *Saccharomyces cerevisiae* for Production of Fuels and Chemicals. ACS Synth. Biol. 4, 332–341. https://doi.org/10.1021/sb500243c

Mehrer, C.R., Incha, M.R., Politz, M.C., Pfleger, B.F., 2018. Anaerobic production of medium-chain fatty alcohols via a β-reduction pathway. Metab. Eng. 48, 63–71. https://doi.org/10.1016/j.ymben.2018.05.011

Mehrer, C.R., Rand, J.M., Incha, M.R., Cook, T.B., Demir, B., Motagamwala, A.H., Kim, D., Dumesic, J.A., Pfleger, B.F., 2019. Growth-coupled bioconversion of levulinic acid to butanone. Metab. Eng. 55, 92–101. https://doi.org/10.1016/j.ymben.2019.06.003

Muller, J., MacEachran, D., Burd, H., Sathitsuksanoh, N., Bi, C., Yeh, Y.-C., Lee, T.S., Hillson, N.J., Chhabra, S.R., Singer, S.W., Beller, H.R., 2013. Engineering of *Ralstonia eutroph*a H16 for Autotrophic and Heterotrophic Production of Methyl Ketones. Appl. Environ. Microbiol. 79, 4433–4439. https://doi.org/10.1128/AEM.00973-13

Nie, L., Ren, Y., Schulz, H., 2008. Identification and Characterization of *Escherichia coli* Thioesterase III That Functions in Fatty Acid β-Oxidation. Biochemistry 47, 7744–7751. https://doi.org/10.1021/bi800595f

Park, J., Rodríguez-Moyá, M., Li, M., Pichersky, E., San, K.-Y., Gonzalez, R., 2012. Synthesis of methyl ketones by metabolically engineered *Escherichia coli*. J. Ind. Microbiol. Biotechnol. 39, 1703–1712. https://doi.org/10.1007/s10295-012-1178-x

Srirangan, K., Liu, X., Akawi, L., Bruder, M., Moo-Young, M., Chou, C.P., 2016. Engineering *Escherichia coli* for Microbial Production of Butanone. Appl. Environ. Microbiol. 82, 2574–2584. https://doi.org/10.1128/AEM.03964-15

Voelker, T.A., Davies, H.M., 1994. Alteration of the specificity and regulation of fatty acid synthesis of *Escherichia coli* by expression of a plant medium-chain acyl-acyl carrier protein thioesterase. J. Bacteriol. 176, 7320–7327. https://doi.org/10.1128/jb.176.23.7320-7327.1994

Wang, F., Langley, R., Gulten, G., Wang, L., Sacchettini, J.C. 2007. Identification of a type III thioesterase reveals the function of an operon crucial for Mtb virulence. Chem. Biol. 14, 543-551

Yan, Q., Pfleger, B.F., 2019. Revisiting metabolic engineering strategies for microbial synthesis of oleochemicals. Metab. Eng. https://doi.org/10.1016/j.ymben.2019.04.009

Youngquist, J.T., Schumacher, M.H., Rose, J.P., Raines, T.C., Politz, M.C., Copeland, M.F., Pfleger, B.F., 2013. Production of medium chain length fatty alcohols from glucose in *Escherichia coli*. Metab. Eng. 20, 177–186. https://doi.org/10.1016/j.ymben.2013.10.006

Yu, G., Nguyen, T.T.H., Guo, Y., Schauvinhold, I., Auldridge, M.E., Bhuiyan, N., Ben-Israel, I., Iijima, Y., Fridman, E., Noel, J.P., Pichersky, E., 2010. Enzymatic Functions of Wild Tomato Methyl ketone Synthases 1 and 2. Plant Physiol. 154, 67–77. https://doi.org/10.1104/pp.110.157073

Yuzawa, S., Deng, K., Wang, G., Baidoo, E.E.K., Northen, T.R., Adams, P.D., Katz, L., Keasling, J.D., 2017. Comprehensive in Vitro Analysis of Acyltransferase Domain Exchanges in Modular Polyketide Synthases and Its Application for Short-Chain Ketone Production. ACS Synth. Biol. 6, 139–147. https://doi.org/10.1021/acssynbio.6b00176

Yuzawa, S., Mirsiaghi, M., Jocic, R., Fujii, T., Masson, F., Benites, V.T., Baidoo, E.E.K., Sundstrom, E., Tanjore, D., Pray, T.R., George, A., Davis, R.W., Gladden, J.M., Simmons, B.A., Katz, L., Keasling, J.D., 2018. Short-chain ketone production by engineered polyketide synthases in *Streptomyces albus*. Nat. Commun. 9, 4569. https://doi.org/10.1038/s41467-018-07040-0

Zhu, M., Xu, X., Li, Y., Wang, P., Niu, S., Zhang, K., Huang, X., 2019. Biosynthesis of the Nematode Attractant 2-Heptanone and Its Co-evolution Between the Pathogenic Bacterium *Bacillus nematocida* and Non-pathogenic Bacterium *Bacillus subtilis*. Front. Microbiol. 10. https://doi.org/10.3389/fmicb.2019.01489

Zhu, J., Dhammi, A., van Kretschmar, J.B., Vargo, E.L., Apperson, C.S., Michael Roe, R., 2018. Novel use of aliphatic n -methyl ketones as a fumigant and alternative to methyl bromide for insect control. Pest Manag. Sci. 74, 648–657. https://doi.org/10.1002/ps.4749

Zhu, Z., Zhou, Y.J., Krivoruchko, A., Grininger, M., Zhao, Z.K., Nielsen, J., 2017. Expanding the product portfolio of fungal type I fatty acid synthases. Nat. Chem. Biol. 13, 360–362. https://doi.org/10.1038/nchembio.2301

Supplementary Data

Metabolic engineering of β-oxidation to leverage thioesterases for production of 2-heptanone, 2-nonanone and 2-undecanone

Qiang Yan[a,b,1], Trevor R. Simmons[a,1], William T. Cordell[a,b], Néstor J. Hernández Lozada[a], Christian J. Breckner[a], Xuanqi Chen[a], Michael A. Jindra[a], and Brian F. Pfleger [a,b,c,*]

[a] Department of Chemical and Biological Engineering, University of Wisconsin-Madison, Madison, WI 53706, United States

[b] DOE Center for Advanced Bioenergy and Bioproducts Innovation, University of Wisconsin-Madison, Madison, WI 53706, United States

[c] Microbiology Doctoral Training Program, University of Wisconsin-Madison, Madison, WI 53706, United States

[1] Designates authors contributing equally to the manuscript.

* Corresponding author. 3629 Engineering Hall, 1415 Engineering Drive, Madison, WI 53706, United States. Phone: +1 608 890 1940. Fax: +1 608 262-5434. E-mail address: pfleger@engr.wisc.edu.

Supplementary Table 1. Strains and plasmids used in this study

Strain/Plasmid	Genotype	Source
Strains		
E. coli DH5a	F- Φ80*lacZ*ΔM15 Δ(*lacZYA-argF*) U169 *recA1 endA*1 *hsdR*17 (rk-, mk+) *phoA supE44* λ- *thi*-1 *gyrA*96 *relA*1	Invitrogen
NHL17	K12 MG1655 Δ*araBAD* Δ*fadD*::P_{trc}CpFatB1*	(Hernández et al., 2018)
ΔRAI	MG1655 Δ*araBAD* Δ*fadR* Δ*fadA* Δ*fadI*	(Agnew et al., 2012)
ΔRBJ	MG1655 Δ*araBAD* Δ*fadR* Δ*fadB* Δ*fadJ*	(Agnew et al., 2012)
ΔRABIJ	MG1655 Δ*araBAD* Δ*fadR* Δ*fadA* Δ*fadB* Δ*fadI* Δ*fadJ*	(Agnew et al., 2012)
TRS12	NHL17 strain Δ*fadAEIR*	This work
TY34	MG1655 Δ*araBAD* Δ*fadE*::P_{trc}-BTE Δ*fadAB*::trcBTE Δ*ackApta*::P_{trc}-BTEΦ(P_{trc}-*fadD*)	(Youngquist et al., 2013)
Plasmids		
pMP11	pKD46 with constitutively expressed Cas9 and an aTc gRNA targeting the ColE1 origin	This work
pgRNA	Constitutively expressed sgRNA targeting a desired gene	This work
pBTRCK	Trc promoter, pBRR1 origin, Kan^R	(Mehrer et al., 2018)
pBTRCK-CpFatB1*	Trc promoter, containing CpFatB1* an C_8-specific thioesterase mutant isolated in the lab	(Hernández et al., 2018)
pBTRCK-MlACO	Trc promoter, containing Mlut_11700 an Acyl-CoA oxidase from *Micrococcus luteus*	This work
pACYC	Trc promoter, pACYC origin, CmR	(Mehrer et al., 2018)
pACYC-MlACO	Trc promoter, containing Mlut_11700 an Acyl-CoA oxidase from *Micrococcus luteus*	This work
pACYC-AbFadA	Trc promoter, containing ^{Ab}FadA a thiolase from *Alcanivorax borkumensis*	This work
pACYC-MaFadA	Trc promoter, containing ^{Ma}FadA a thiolase from *Marinobacter aquaeolei*	This work
pACYC-SeFadA	Trc promoter, containing ^{Se}FadA a thiolase from *Salmonella enterica*	This work
pACYC-ReBktB	Trc promoter, containing ^{Re}BktB a thiolase from *Ralstonia eutropha*	This work

pACYC-PpFadA	Trc promoter, containing ^{Pp}FadA a thiolase from *Pseudomona putida*	This work
pACYC-EcFadA	Trc promoter, containing ^{Ec}FadA a thiolase from *E. coli*	This work
pACYC-VfFadA	Trc promoter, containing ^{Vf}FadA a thiolase from *Vibrio fisheri*	This work
pACYC-AbFadB	Trc promoter, containing ^{Ab}FadB a bi-functional 3-hydroxyacyl-CoA dehydrogenase from *Alcanivorax borkumensis*	This work
pACYC-MaFadB	Trc promoter, containing ^{Ma}FadB a bi-functional 3-hydroxyacyl-CoA dehydrogenase from *Marinobacter aquaeolei*	This work
pACYC-SeFadB	Trc promoter, containing ^{Se}FadB a bi-functional 3-hydroxyacyl-CoA dehydrogenase from *Salmonella enterica*	This work
pACYC-PpFadB	Trc promoter, containing ^{Pp}FadB a bi-functional 3-hydroxyacyl-CoA dehydrogenase from *Pseudomona putida*	This work
pACYC-EcFadB	Trc promoter, containing ^{Ec}FadB a bi-functional 3-hydroxyacyl-CoA dehydrogenase from *E. coli*	This work
pACYC-VfFadB	Trc promoter, containing ^{Vf}FadB a bi-functional 3-hydroxyacyl-CoA dehydrogenase from *Vibrio fisheri*	This work
pTRC99a	Trc promoter, pBR322 origin, AmpR	(Mehrer et al., 2018)
pTRC99a-FadD6-BaFadM	Trc promoter, fadD6 from *Mycobacterium tuberculosis* in front of FadM (GI: WP_034493719) from *Buttiauxella agrestis*	
pTRC99a-FadD6-BbFadM	Trc promoter, fadD6 in front of FadM (GI: KGQ11242) from *Beauveria bassiana*	
pTRC99a-FadD6-EclFadM	Trc promoter, fadD6 in front of FadM (GI: CZU17062) from *Enterobacter cloacae*	
pTRC99a-FadD6-CtFadM	Trc promoter, fadD6 in front of FadM (GI: WP_012815543) from *Cronobacter turicensis*	This Work
pTRC99a-FadD6-EcFadM	Trc promoter, fadD6 in front of FadM (GI: WP_001194534) from *E. coli*	
pTRC99a-FadD6-Mt1FadM	Trc promoter, FadD6 in front of fadM1 (GI: WP_046024041) from *Mycobacterium tuberculosis*	This Work

pTRC99a-FadD6-Mt2FadM	Trc promoter, FadD6 in front of FadM2 (GI: WP_063014014) from *M. tuberculosis*	This Work
pTRC99a-FadD6-Mt3FadM	Trc promoter, FadD6 in front of FadM3 (GI: WP_066852574) from *M. tuberculosis*	This Work
pTRC99a-FadD6-Mt4FadM	Trc promoter, FadD6 in front of FadM4 (GI: WP_076060981)from *M. tuberculosis*	This Work
pTRC99a-FadD6-Mt5FadM	Trc promoter, FadD6 in front of FadM5 (GI: WP_090604673) from *M. tuberculosis*	This Work
pTRC99a-FadD6-MuFadM	Trc promoter, FadD6 in front of FadM (GI: WP_036160439) from *Marinomonas ushuaiensis*	This Work
pTRC99a-FadD6-NgFadM	Trc promoter, FadD6 in front of FadM (GI: WP_113852040) from *Neisseria gonorrhoeae*	This Work
pTRC99a-FadD6-PaFadM	Trc promoter, FadD6 in front of FadM (GI: WP_141239354) from *Pseudomonas aeruginosa*	This Work
pTRC99a-FadD6-PsFadM	Trc promoter, FadD6 in front of FadM (GI: WP008916720) from *Providencia sneebia*	This Work
pTRC99a-FadD6-SeFadM	Trc promoter, FadD6 in front of FadM (GI: EBS6353971) from *Samonella enterica*	This Work
pTRC99a-FadD6-SoFadM	Trc promoter, FadD6 in front of FadM (GI: WP_004954593) from *Serratia odorifera*	This Work

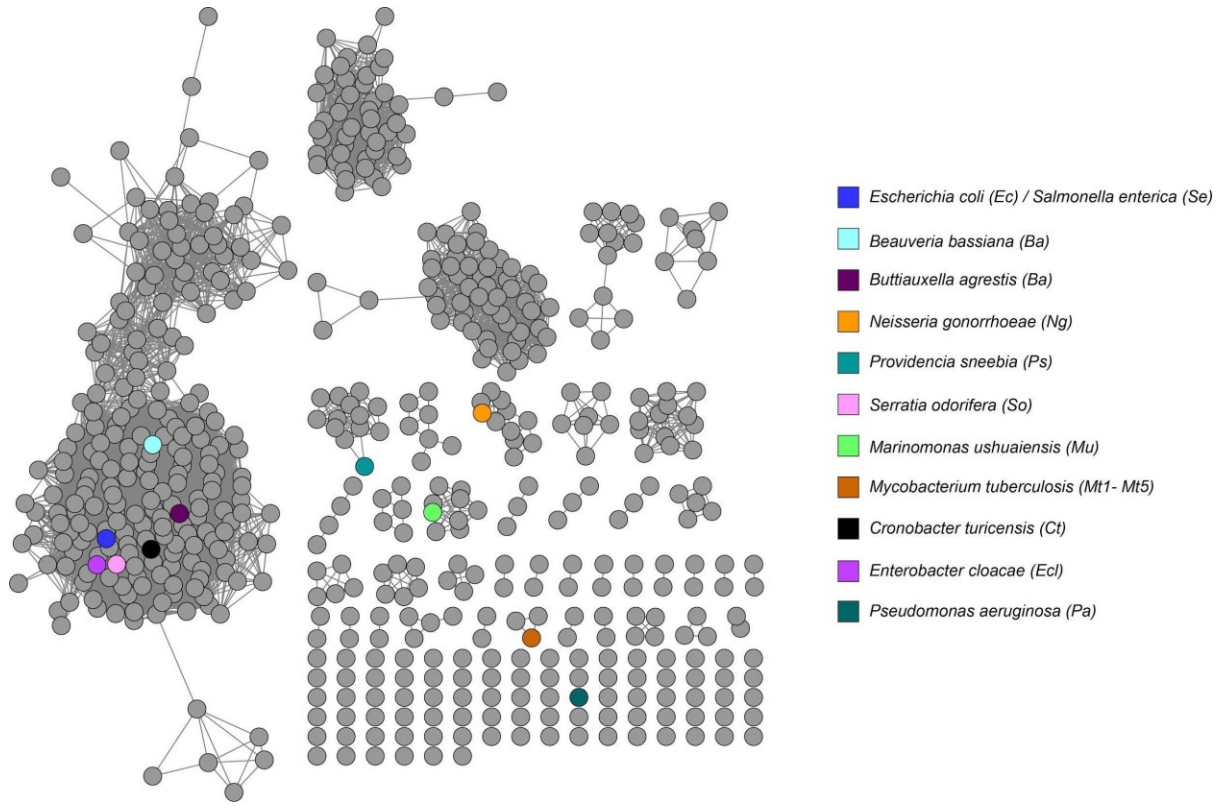

		EcFadM	SeFadM	CsFadM	CtFadM	BbFadM	BaFadM	SoFadM	MtFadM1	PsFadM	NgFadM	MuFadM	MtFadM2	PaFadM	MtFadM3	MtFadM4	MtFadM5
Escherichia coli	EcFadM	100	95	91	87	82	82	76	58	48	41	39	31	30	26	24	24
Salmonella enterica	SeFadM	95	100	93	89	80	79	77	58	50	45	45	35	38	30	28	28
Cucumis sativus	CsFadM	91	93	100	88	82	82	77	57	48	43	42	33	32	28	24	25
Cronobacter turicensis	CtFadM	87	89	88	100	78	80	76	57	51	41	41	31	31	26	26	24
Beauveria bassiana	BbFadM	82	80	82	78	100	94	80	55	44	43	38	29	32	27	24	24
Buttiauxella agrestis	BaFadM	82	79	82	80	94	100	77	53	46	41	38	30	34	28	25	25
Serratia odorifera	SoFadM	76	77	77	76	80	77	100	55	49	41	39	26	31	25	25	25
Mycobacterium tuberculosis	MtFadM1	58	58	57	57	55	53	55	100	45	33	37	25	33	26	44	44
Providencia sneebia	PsFadM	48	50	48	51	44	46	49	45	100	36	36	26	30	34	36	35
Neisseria gonorrhoeae	NgFadM	41	45	43	41	43	41	41	33	36	100	40	30	26	33	26	37
Marinomonas ushuaiensis	MuFadM	39	45	42	41	38	38	39	37	36	40	100	28	30	37	26	30
Mycobacterium tuberculosis	MtFadM2	31	35	33	31	29	30	26	25	26	30	28	100	25	25	24	36
Pseudomonas aeruginosa	PaFadM	30	38	32	31	32	34	31	33	30	26	30	25	100	28	25	36
Mycobacterium tuberculosis	MtFadM3	26	30	28	26	27	28	25	26	34	33	37	25	28	100	74	70
Mycobacterium tuberculosis	MtFadM4	24	28	24	26	24	25	25	44	36	26	26	24	25	74	100	84
Mycobacterium tuberculosis	MtFadM5	24	28	25	24	24	25	25	44	35	37	30	36	36	70	84	100

Figure S1. Sequence similarity of FadM homologs (Top). Cluster representation of sequence identity generated using the Enzyme Similarity Tool. A node representing a protein sequence, an edge, which refers to a line connecting between two nodes, representing two connected nodes share similar sequences, clusters representing nodes fall into the different protein families. (Bottom) Pairwise amino acid identity (%) between FadM homologs.

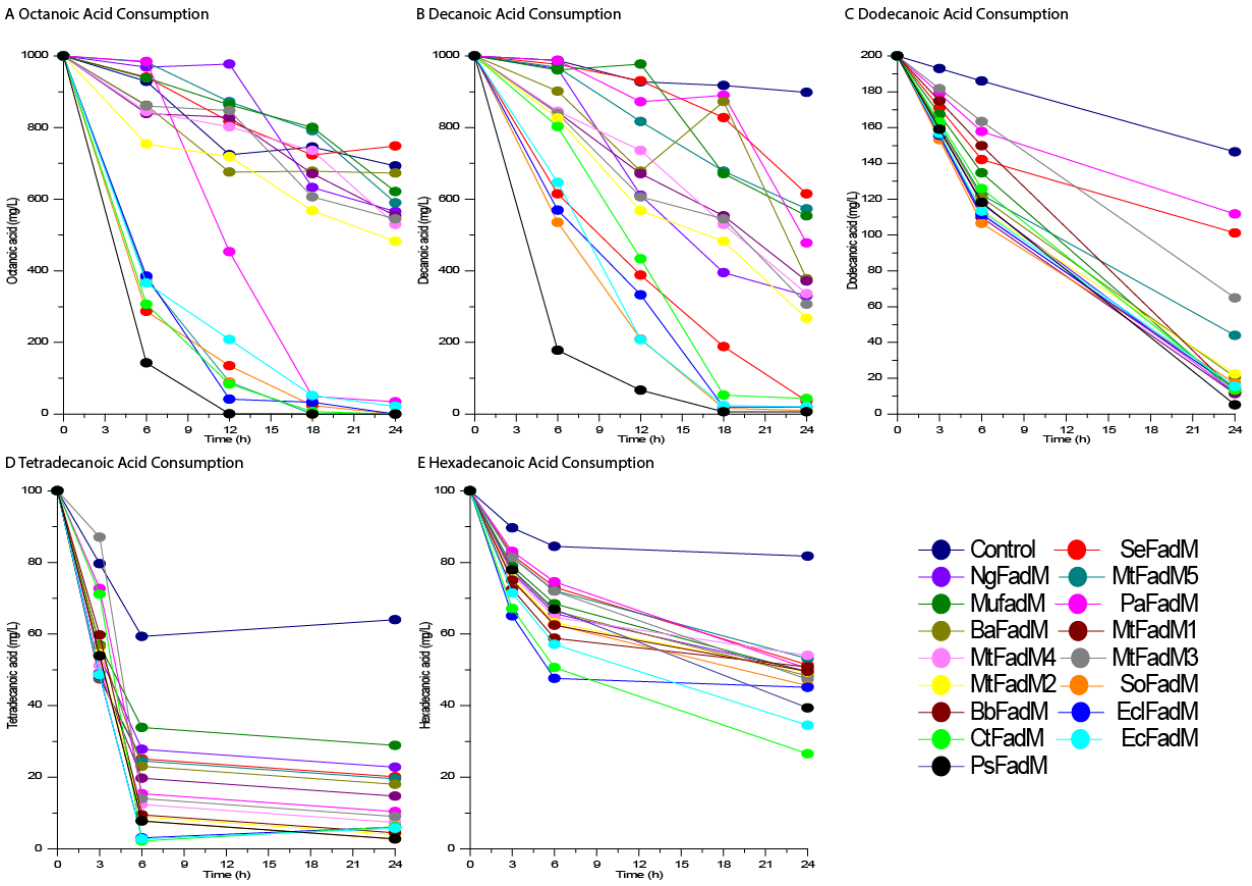

Figure S2. Timecourse of fatty acid consumption experiments used to calculate the consumption rates presented in Figure 2. Cells were fed 1 g/L octanoic acid, 1 g/L decanoic acid 200 mg/L dodecanoic acid, 100 mg/L tetradecanoic acid, or 100 mg/L hexadecanoic acid. Each dot represented values calculated from three biological replicates. Fatty acid consumption rate (mg/L/h) was calculated by following equation:

Fatty acid consumption rate (mg/L/h) = (Initial FFA concentration (mg/L) - FFA concentration (mg/L) at T time point)/Time T (h), where T equals to 6 hrs for octanoic acid and decanoic acid, and T equals to 3 hrs for dodecanoic acid, tetradecanoic acid, and hexadecanoic acid.

Addressing Methyl Ketone Quantification

When producing volatile products, like methyl ketones, loss due to vaporization tends to increase with shorter the acyl chain lengths. This trend for methyl ketones is represented in **Figure S3B** where the relative vapor pressure can increase drastically even with only a single acyl carbon difference. To assess the potential loss of the target product, we performed shake flask experiments with a known starting concentration of 2-heptanone, 2-nonanone, 2-undecanone. We found that the majority of methyl ketones were lost over 48 hours, however the addition of 20% v/v dodecane overlay reduced the loss to 10-30% depending on chain length **(Figure S3A)**. For this reason, all methyl ketone production experiments were done with at least a 10% v/v dodecane overlay.

Although methyl ketone vaporization in shake flask experiments was minimized by the addition of dodecane, open systems like bioreactors can suffer from additional loss due to sparged gas stripping the product. In addition to a 20% (v/v) dodecane overlay, we attempted further reduce product loss in our bioreactor experiments by condensing evaporated methyl ketones in the off-gas with an external water cooling condenser **(Figure S4)**. Some methyl ketones were captured (~5% of total titer for 2-heptanone and < 1% for 2-nonanone), however there was likely still significant product loss due to stripping when considering the previous evaporation flask experiments. This result suggests that the retention time, temperature or both were not sufficient to capture most of the methyl ketones in the offgas. Addressing volatility continues to be a challenge for microbial production, and we hope these results serve as an example of the significant losses that can occur and how to improve methods for product capture in future experiments.

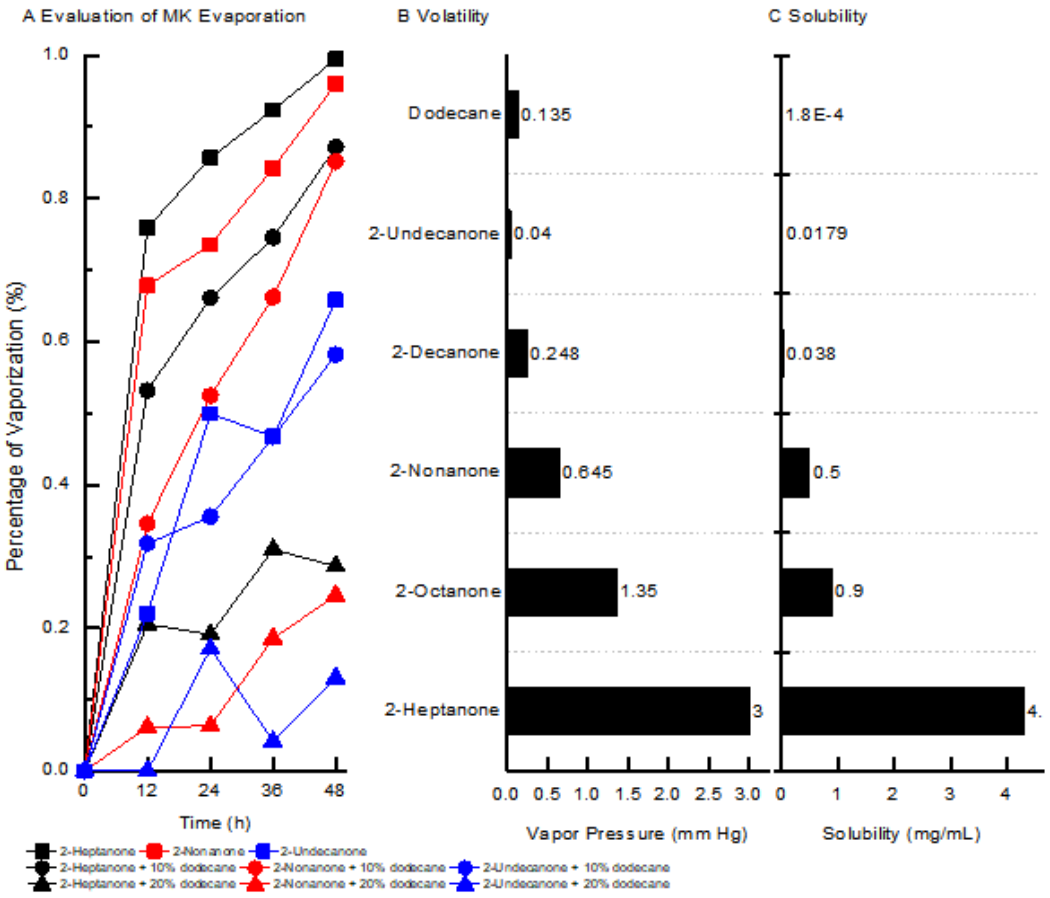

Figure S3 Evaluation of methyl ketone evaporation. (A) 2-heptanone, 2-nonanone and 2-undecanone evaporation was tracked over time to understand evaporation behavior in aerobic conditions. (B) Reported values of vapor pressure of MK and dodecane from PubChem (https://pubchem.ncbi.nlm.nih.gov/). Vapor pressure represents the tendency of molecules and atoms to escape from a liquid phase. With exception of reported 2-heptanone vapor pressure measured at 20°C, all reported molecules vapor pressures were measured at 25°C. (C) Reported values of solubility of MK and dodecane in water from PubChem. all reported solubility values were measured at 25 or 30°C.

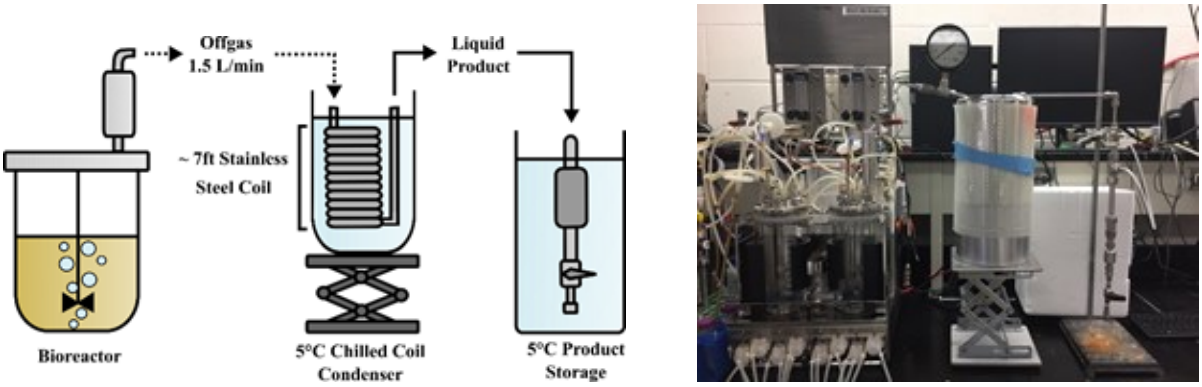

Figure S4. (left) Schematic view of the vapor capture system. During fermentation, the bioreactor off-gas flows at 1.5 L/min through a ~7 ft stainless steel coiled condenser and the condensed product is then collected in a stainless-steel holding vessel. Both the condenser and collector are submerged in a water-ice bath and cooled by a 5°C water line from a separate water cooler. Final condensed products can be released from the collector by opening a ball valve. (right) Vapor condenser setup attached to the bioreactor system.

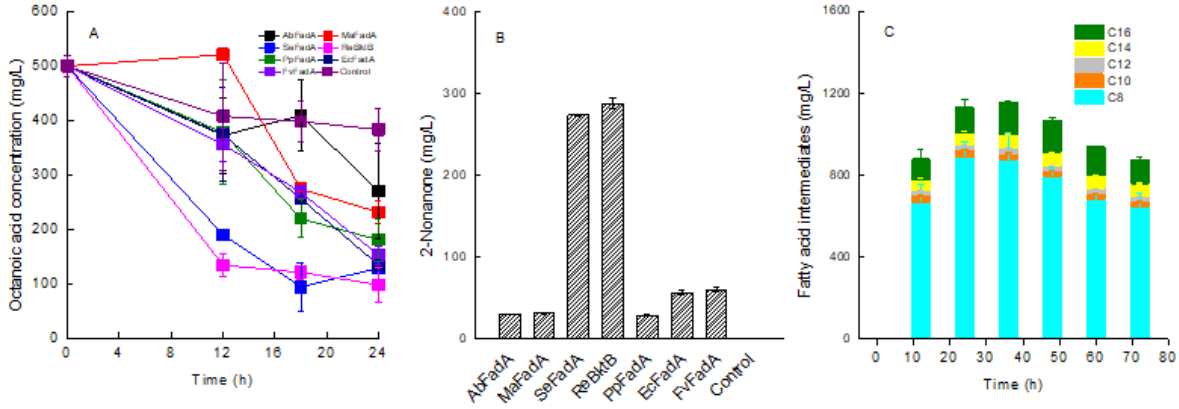

Figure S5 Bioprospecting thiolase variants for use in producing β-ketoacyl-CoAs (A) Time course of octanoic acid consumption and (B) 2-nonanone production when feeding 500 mg/L octanoic acids to cultures of straintrain *E. coli* Δ*fadRABIJ* expressing pACYC-"fadA" + pTRC99a-FadD6-*Ps*FadM + pBTRCK-*Cp*FatB1* (C) Residual free fatty acid titers over time during growth of *E. coli* Δ*fadABIJR* ptrc99a-PsfadM-fadD6 + pACYC-ReBktB+ pBTRCK-*Cp*FatB1* in 250 mL shake flasks containing 50 mL Clomburg medium with 45 g/L glycerol (from experiment in **Figure 5**).

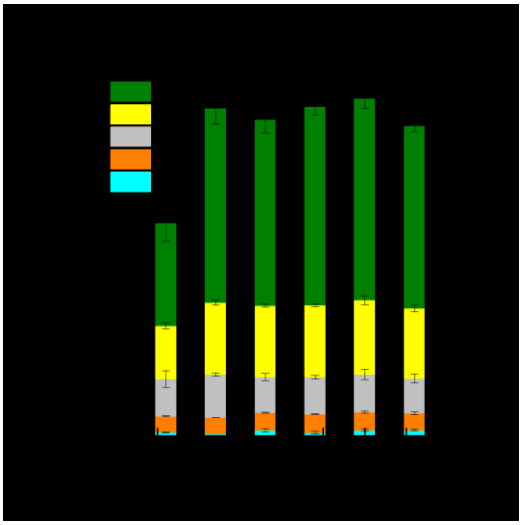

Figure S6 Residual free fatty acid titers over time during growth of *E. coli* TY34 strain + pACYC-PpFadB + pTRC99a-PsFadM from experiment described in **Figure 6**

Supplementary References.

Agnew, D.E., Stevermer, A.K., Youngquist, J.T., Pfleger, B.F., 2012. Engineering Escherichia coli for production of C12–C14 polyhydroxyalkanoate from glucose. Metab. Eng. 14, 705–713. https://doi.org/10.1016/j.ymben.2012.08.003

Hernández Lozada, N.J., Lai, R.-Y., Simmons, T.R., Thomas, K.A., Chowdhury, R., Maranas, C.D., Pfleger, B.F., 2018. Highly Active C 8 -Acyl-ACP Thioesterase Variant Isolated by a Synthetic Selection Strategy. ACS Synth. Biol. 7, 2205–2215. https://doi.org/10.1021/acssynbio.8b00215

Mehrer, C.R., Incha, M.R., Politz, M.C., Pfleger, B.F., 2018. Anaerobic production of medium-chain fatty alcohols via a β-reduction pathway. Metab. Eng. 48, 63–71. https://doi.org/10.1016/j.ymben.2018.05.011

Youngquist, J.T., Schumacher, M.H., Rose, J.P., Raines, T.C., Politz, M.C., Copeland, M.F., Pfleger, B.F., 2013. Production of medium chain length fatty alcohols from glucose in Escherichia coli. Metab. Eng. 20, 177–186. https://doi.org/10.1016/j.ymben.2013.10.006